Max-Planck-Institut für Sonnensystemforschung
Katlenburg-Lindau, Germany

Nonlinear force-free magnetic field extrapolations: Comparison of Grad-Rubin and Wheatland-Sturrock-Roumeliotis algorithms

Bernd Inhester, Thomas Wiegelmann
Max-Planck-Institute für Sonnensystemforschung
37191 Katlenburg-Lindau, Germany

Abstract

We compare the performance of two alternative algorithms for force-free magnetic field extrapolations given suitable boundary conditions. For this comparison, we have implemented both algorithms on the same finite element grid which uses Whitney forms to describe the fields within the grid cells. The additional use of conjugate gradient and multigrid iterations result in quite effective codes.
The Grad-Rubin and Wheatland-Sturrock-Roumeliotis algorithms both perform well for the reconstruction of a known analytic force-free field. For more arbitrary boundary conditions the Wheatland-Sturrock-Roumeliotis approach has some difficulties because it requires overdetermined boundary information which may include inconsistencies. The Grad-Rubin code on the other hand loses convergence for strong current densities. For the example we have investigated, however, the maximum possible current density seems to be not far from the limit beyond which a force free field cannot exist anymore for a given normal magnetic field intensity on the boundary.

The grid: regular 3D Whitney forms

Whitney forms can be considered as the finite element discrete counterpart to differential forms in continuous vector calculus (Bossavit, 1988)

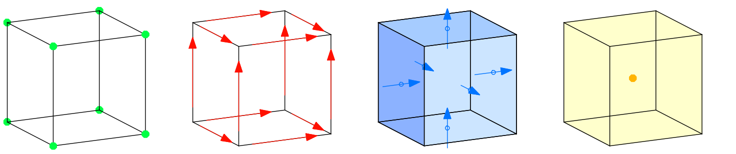

0-form	1-form	2-form	3-form
Lagrange element for scalars $\in \mathbb{R}$	Nédélec element for $\mathbb{H}$(curl)	Raviart-Thomas element for $\mathbb{H}$(div)	FV element for scalars $\in \mathbb{R}$

The Nédélec and Raviart-Thomas elements are also known as edge elements because field components are defined on the edges and faces of the grid cell (Nédelec, 1986; Raviart and Thomas, 1977). Fields are mapped naturally from a n-form to an $(n+1)$-form by exterior differentiation:

$$\text{0-form} \xrightarrow{\text{grad}} \text{1-form} \xrightarrow{\text{curl}} \text{2-form} \xrightarrow{\text{div}} \text{3-form}$$

• The big advantage: All common differential operators can be represented as exterior differentiations on forms. Double differentiations give zero exactly, e.g.,

$$\text{curl} \circ \text{grad} \equiv \text{div} \circ \text{curl} \equiv 0 \; ,$$

div and grad are adjoint operations
The introduction of a dual grid allows a natural relationship between n-forms of the primal grid and $(3-n)$-forms of the dual grid

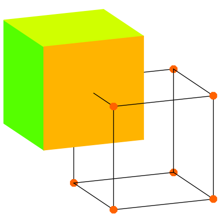

In this setting, an n-form of the primal grid has the same representation as the $(3-n)$-form on the dual grid and vice versa, but element shape functions are different.
The Hodge (or *)-transform between primal and dual grid only results in a change of the shape function.
The final pattern (complex) of forms together with mappings among them:

$$\begin{array}{ccccccc}
\text{primal grid} & \text{0-form} & \xrightarrow{\text{grad}} & \text{1-form} & \xrightarrow{\text{curl}} & \text{2-form} & \xrightarrow{\text{div}} & \text{3-form} \\
 & \updownarrow * & & \updownarrow * & & \updownarrow * & & \updownarrow * \\
\text{dual grid} & \text{3-form} & \xleftarrow[\text{div}]{} & \text{2-form} & \xleftarrow[\text{curl}]{} & \text{1-form} & \xleftarrow[\text{grad}]{} & \text{0-form}
\end{array}$$

The formation of more involved differential operations is obvious. E.g., the common 7-point stencil Laplacian can be represented as:

$$\text{for a 0-form:} \qquad \Delta = * \circ \text{div} \circ * \circ \text{grad}$$

$$\text{for a 1-form:} \qquad \Delta = \text{grad} \circ * \circ \text{div} \circ * - * \circ \text{curl} \circ * \circ \text{curl}$$

The boundary value problem

The magnetic field in some domain V of the corona may be described by

$$\boldsymbol{\nabla} \cdot \boldsymbol{B} = 0 \; ; \quad \boldsymbol{\nabla} \times \boldsymbol{B} = \boldsymbol{j} \; ; \quad \boldsymbol{j} \times \boldsymbol{B} = 0 \tag{1}$$

The alignment of current and magnetic field causes the problem to be nonlinear, hence the questions which boundary information is to be supplied and how to solve (1) are by no means trivial.

Boundary conditions which seem necessary and sufficient for (1) are (Boulmezaoud and Amari, 2000)

$$\begin{aligned} &\boldsymbol{n} \cdot \boldsymbol{B} \text{ on the whole boundary } \partial V \\ &\boldsymbol{n} \cdot \boldsymbol{\nabla} \times \boldsymbol{B} \text{ on either } (\partial V)^- \text{ or } (\partial V)^+ \end{aligned} \tag{2}$$

where $(\partial V)^{\pm}$ is that part of the surface of V where $\boldsymbol{n} \cdot \boldsymbol{B}$ is either > 0 or < 0.

But not the all boundary values which comply with (2) are allowed:
• diff flux conservation on every $S(\alpha) \subset \partial V$ where α is any const

$$\int_{S(\alpha)} B_n d^2x = 0$$

• Maxwell's stresses on ∂V must vanish (Molodensky, 1966)

$$\int_{\partial V} (2B_n^2 - B^2)\, d^2x = 0 \; , \qquad \int_{\partial V} B_i B_j \, d^2x = 0 \;\text{ for } i \neq j$$

Grad-Rubin iteration by means of Whitney forms

The iteration algorithm by Grad and Rubin (1958) is:

$\Delta\phi = 0$ `with BC` $\partial_n\phi = B_n$
$\mathbf{B}^{(0)} = \mathrm{grad}\,\phi$
`do until convergence`
    `integrate` $\alpha^{(n)}$ `from` $\mathbf{B}^{(n)}\cdot\nabla\alpha^{(n)} = 0$
    $\delta\boldsymbol{j} = \boldsymbol{\nabla}\times\boldsymbol{B}^{(n)} - \alpha^{(n)}\boldsymbol{B}^{(n)}$
    `solve` $\Delta\,\delta\boldsymbol{A} = \delta\boldsymbol{j}$ `with BC` $\boldsymbol{n}\times\delta\boldsymbol{A} = 0,$
        `and` $(\boldsymbol{n}\cdot\boldsymbol{\nabla})\,\delta A_n = 0$
    $\boldsymbol{B}^{(n+1)} = \boldsymbol{B}^{(n)} + \boldsymbol{\nabla}\times\delta\boldsymbol{A}$
`end do`

Discretized as Whitney forms, the scheme looks as follows:

$$\begin{tikzcd}[column sep=large]
\text{primal grid} & \underset{\text{0-form}}{\phi} \arrow[r, "\text{grad}"] & \underset{\text{1-form}}{\mathbf{B}} \arrow[r, "\text{curl }-\alpha\cdot"] & \underset{\text{2-form}}{\delta\mathbf{j}} \arrow[r, "\text{div}"] \arrow[d, "\Delta^{-1}"] & \underset{\text{3-form}}{0} \\
\text{dual grid} & & \underset{\delta\mathbf{B}}{\text{2-form}} \arrow[u, "+"] & \underset{\delta\mathbf{A}}{\text{1-form}} \arrow[l, "\text{curl}"] &
\end{tikzcd}$$

The critical operation is $\alpha\cdot$. It includes:

- the integration of $\mathbf{B}\cdot\nabla\alpha = 0$ with the current magnetic field iterate. As boundary condition we take a weighted average of observed/assumed α from both ends of the field line.
- the step $\delta\mathbf{j} = \alpha\cdot\mathbf{B}$ then includes the mapping from a 1-form to a 2-form as the only interpolation of the algorithm.

Wheatland-Sturrock-Roumeliotis iteration by means of Whitney forms

The algorithm proposed by Wheatland, Sturrock and Roumeliotis (2000) tries to find the force-free field $\boldsymbol{B}$ from

$$\boldsymbol{B} = \mathrm{argmin}(L)\,, \quad L(\boldsymbol{B}) = \int_V |w\,\boldsymbol{j}\times\boldsymbol{B}|^2 + \int_V |\boldsymbol{\nabla}\cdot B|^2$$

The discretized integrals are Hilbert products for 3-forms.
For the minimization of L we use a specially designed CG algorithm:

- Exact line search at each iteration step along the search direction $\delta\boldsymbol{B}^{(i)}$
- New search direction $\delta\boldsymbol{B}^{(i+1)}$ chosen from H-orthogonality: $\delta\boldsymbol{B}^{(i+1)}\boldsymbol{H}\delta\boldsymbol{B}^{(i)} = 0$ where $\boldsymbol{H}$ is the local Hessian.

Convergence speed scales with 1/(grid size) :

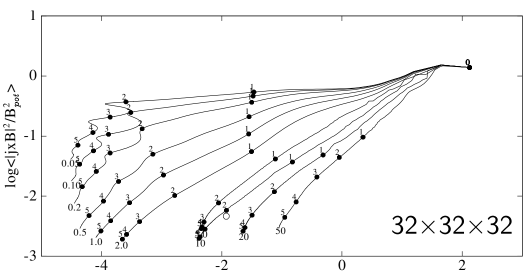

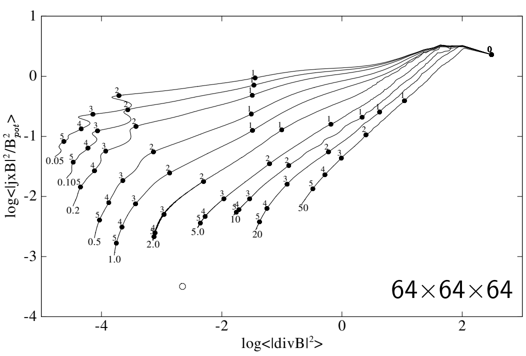

Numerical Results

To reconstruct a Low and Lou (1990) solution with exact boundary values the Grad-Rubin code requires less than 10 iterations, the Wheatland-Sturrock-Roumeliotis scheme ~100 iteration steps to reduce the mean square Lorentz force to a value of the discretization error. The Grad-Rubin code performs slightly faster for comparable problems.

Grad-Rubin   Wheatland-et-al

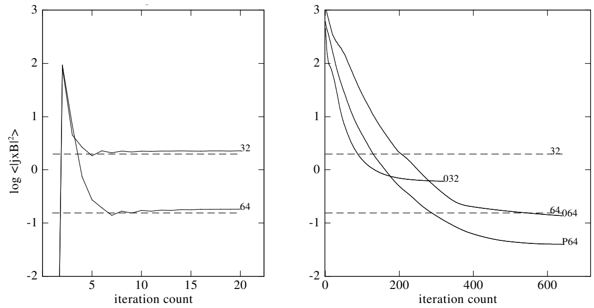

The dashed lines denote the respective residual Lorentz force for the discretized Low and Lou (1990) solution $\boldsymbol{B}_{\mathrm{org}}$.
Representative field lines of the Low and Lou (1990) field reconstruction:

Original   Wheatland-et-al without weight

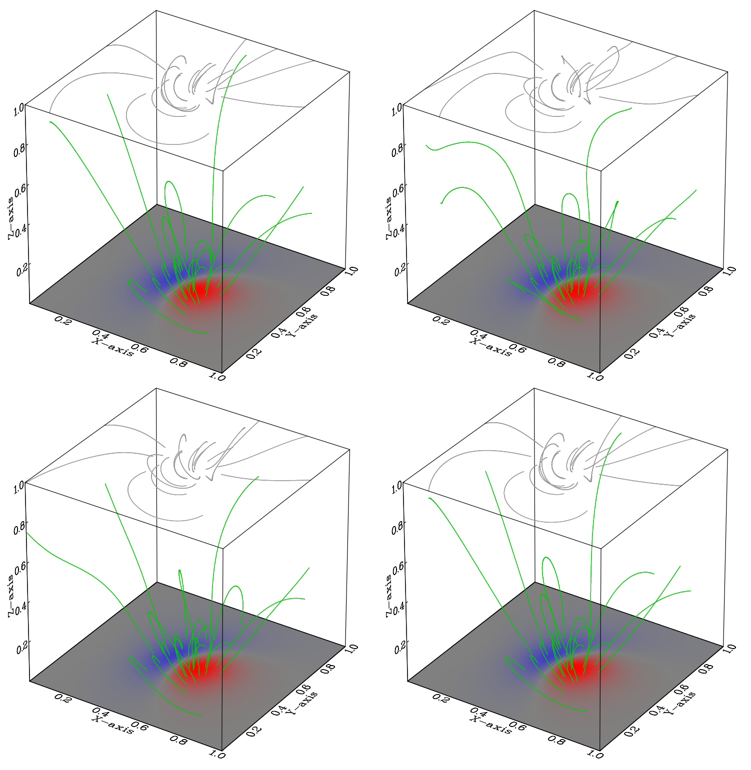

Wheatland-et-al with weight   Grad-Rubin

The colour code at the bottom represents B_z, the top plane shows the vertical projection of the field lines.
The mean square error to the original Low and Lou (1990) field with iteration count:

Grad-Rubin   Wheatland-et-al

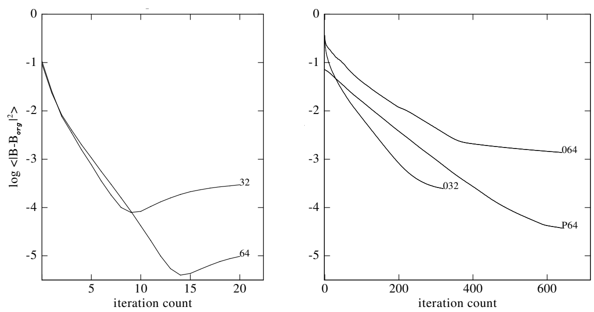

How does the magnetic field help us with stereoscopy ?

The magnetic field may serve as an important constraint to resolve some of the ambiuities in the stereo reconstruction of coronal loops. We will use the magnetic field reconstructions to identify the loops in the STEREO images (matching problem) and resolve the stereo ambiguity.
The precedure, we have in mind is:

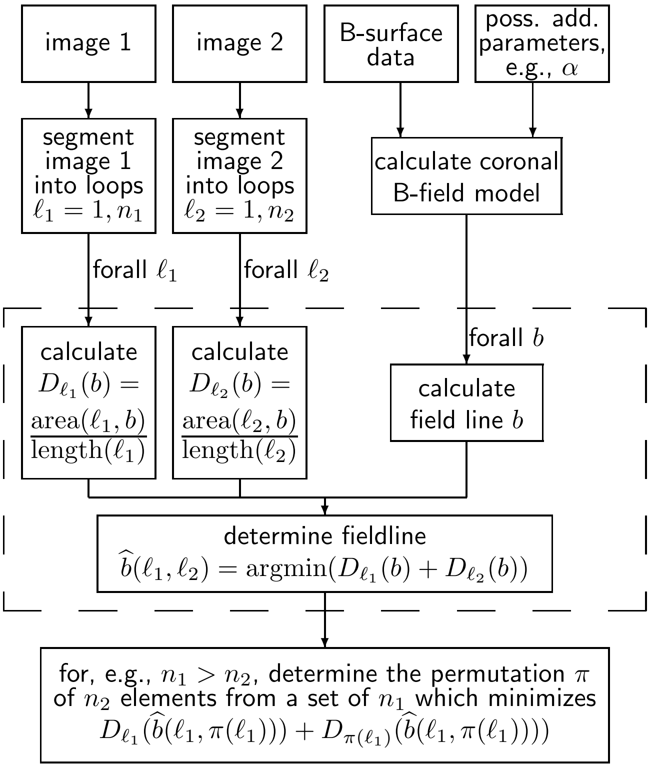

The segmentation into loops will be done by ridge detectors (Lindeberg, 1998) or the Oriented Connectivity Method of Lee et al. (2004). The distance measure $D_\ell(b)$ between a loop curve ℓ found by one of these methods and a projected magnetic field line b mybe replaced by alternative measures.
As a result we receive a permutation $\ell_1 \rightarrow \ell_2 = \pi(\ell_1)$ which tells us the association between loops in image 1 and 2.

A simple example

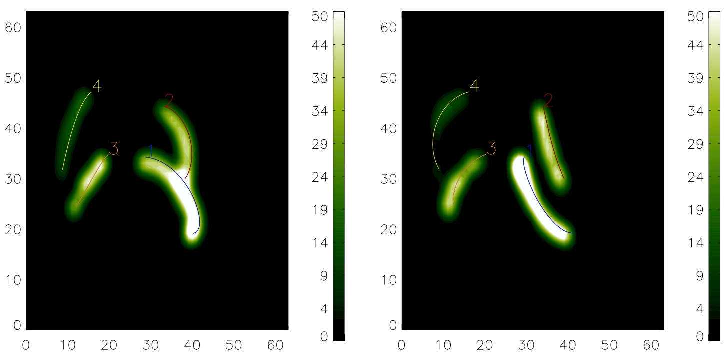

Test loops as seen from two points of view and their segmentation into curves $\ell_1 = 1, 4$ and $\ell_2 = 1, 4$.

The knowledge of the right loop associations removes the ghost features which arise when wrong associations (see stereoscopy I below) between loops are used.
Even a bad magnetic field model may give the right association: here all models (a to c) gave the right result:

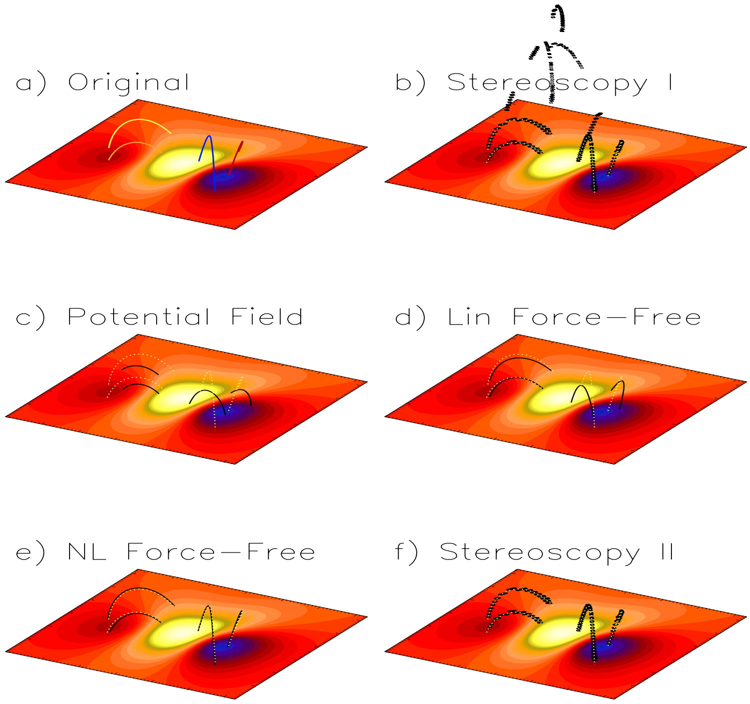

a) Model field lines to be reconstructed
b) Straight forward stereoscopic reconstruction regardless of loop associations
c-e) Optimal field lines $\widehat{b}(\ell_1, \pi(\ell_1))$ for different magnetic field models
b) Stereoscopic reconstruction only of loops associated by $\ell_1 \rightarrow \ell_2 = \pi(\ell_1)$

References

A. Bossavit, Mixed finite elements and the complex of Whitney forms. In J. Whiteman, editor, *The mathematics of finite elements and applications VI*, pages 137–144. Academic Press, London, 1988.

T. Z. Boulmezaoud and T. Amari, On the existence of non-linear force-free fields in three-dimensional domains. *Zeitschrift für angewandte Mathematik und Physik*, 51:942–967, 1999.

H. Grad and H. Rubin, Hydromagnetic equilibria and force-free magnetic fields. In *Proc. 2nd. Intern. Conf. on Peaceful Uses of Atomic Energy*, volume 31. United Nations, Geneva, Switzerland, 1958.

J. K. Lee, T. S. Newman and G. A. Gary, Automated detection of solar loops by the Oriented Connectivity Method *17th Intern. Conference on Pattern Recognition*, Cambridge, 2004

T. Lindeberg Edge detection and ridge detection with automatic scale selection *International Journal of Computer Vision*, 30(2), 117–154, 1998

B. C. Low and Y. Q. Lou, Modeling solar for force-free magnetic fields. *Astrophysical Journal*, 352:343–352, 1990.

M. M. Molodensky, Integral properties of force-free fields. *Soviet Astronomy*, 12:585–588, 1969.

J. C. Nédélec, A new family of mixed finite elements in $\mathbb{R}^3$. *Numerische Mathematik*, 50:57–81, 1986.

P. A. Raviart and J. M. Thomas, *A mixed finite element method for second order elliptic problems*, volume 606 of *Lecture Notes in Mathematics*. Springer Verlag, 1977.

M. S. Wheatland, P. A. Sturrock, and G. Roumeliotis, An Optimization Approach to Reconstructing Force-free Fields. *Astrophysical Journal*, 540:1150–1155, 2000.